Manuscript ID: MRSCOM-2020-0070_R1

Submission to ***MRS Communications***

3D Printed Porous Tissue Engineering Scaffolds with the Self-folding Ability and Controlled Release of Growth Factor

Jiahui Lai, Junzhi Li, Min Wang *

Department of Mechanical Engineering
The University of Hong Kong
Pokfulam Road, Hong Kong

Keywords: *3D printing, tissue engineering, shape morphing scaffold, self-folding, growth factor, controlled release*

* Corresponding Author:
Professor Min Wang, at the University of Hong Kong, Hong Kong
Email: memwang@hku.hk Tel: +852 3917 7903 Fax: +852 2858 5415

Abstract

This study investigated a new strategy for fabricating porous scaffolds with the self-folding ability and controlled release of growth factors via 3D printing. The scaffolds were a bilayer structure comprising a poly(D,L-lactide-co-trimethylene carbonate) scaffold for providing the shape morphing ability and a gelatin methacrylate scaffold for encapsulating and delivering growth factor. The structure, shape morphing behaviour, growth factor release and its effect on stem cell behaviour were studied for new scaffolds. The results suggest that these scaffolds have great potential for regenerating tissues such as blood vessels. This work also contributes to developments of 3D printing in tissue engineering.

1. Introduction

Scaffold-based tissue engineering provides a major approach for regenerating human body tissues in which bioactive biomolecules can be loaded into the scaffold matrix or onto the surface of scaffold struts for enhancing tissue regeneration [1]. Porous scaffolds mimicking the natural extracellular matrix of human body tissues can serve well as a substrate for cell attachment, proliferation and differentiation and facilitate new tissue formation *in vivo*. The architecture (pore size, shape, interconnectivity, porosity, etc.) and properties (physical, biological and mechanical) of scaffolds should be carefully controlled to best regenerate the target tissue [2].

3D printing is a manufacturing platform developed since 1986 when the first 3D printing technology – stereolithography (SLA) – was patented [3]. It is an additive manufacturing process where materials are deposited in a layer-by-layer manner to construct 3D objects. It presents a very attractive manufacturing platform and has been applied in many and diverse areas such as electronic devices, energy, food industry, and art creation [4]. The powerful technologies of 3D printing have also been employed in the tissue engineering field for fabricating various porous scaffolds through precisely placing biomaterials, biomolecules or even living cells in the scaffolds [5, 6]. At present, although 3D printing has been used to fabricate tubular hollow structures for tissue engineering applications, it still has difficulties to produce tubular porous hollow scaffolds with a good control over their diameters. Currently, there are mainly three approaches to fabricate tubular hollow structures: indirect printing by using a sacrificial material, direct printing structures with interconnected channels, and direct printing tubular hollow structures using coaxial nozzles. However, none of these methods can simultaneously control accurately the diameter of fabricated tubular hollow structures and achieve desired porosity in tubular hollow structures. 4D printing was

introduced to the public by Tibbits in 2013 [7]. With 4D printing, 3D printed static objects will change their shapes over time, i.e., 4D printing uses 3D printing technologies to produce shape-morphing objects. Such objects can meet the demanding requirements in particularly applications. In recent years, 4D printing using shape memory polymers attracts increasing attention in the tissue engineering field [8, 9]. 4D printing can overcome the difficulties encountered in 3D printing of desired tubular porous scaffolds. Through 4D printing, a 2D planar porous scaffold with the self-folding ability can be fabricated first, followed by shape transformation under suitable external stimuli, resulting in a tubular porous scaffold. Such shape morphing scaffolds will have the advantage of achieving homogenous cell distribution on 3D tubular scaffolds. Cell seeding after scaffold fabrication has been the main approach to load cells into scaffolds. This method may evenly distribute cells onto 2D planar scaffolds; but it has the difficulty to form a homogenous monolayer of cells (especially endothelial cells) onto a 3D tubular structure. With 4D printing, cells can be seeded onto scaffolds in their temporary 2D shape, followed by self-folding of the scaffolds into tubular shape upon suitable stimuli, thereby achieving a homogenous cell distribution on the 3D tubular scaffolds. Currently, materials used in 3D printing of shape morphing structures are either shape memory polymers which can undergo shape change upon heating or hydrogels which can undergo volume change upon immersion in water [10-12]. Shape memory polymers are synthetic polymers which exhibit good mechanical properties and structural integrity but a lower degree of biocompatibility, whereas natural hydrogels exhibit much better biocompatibility but poor mechanical properties. To promote the regeneration of new body tissues, growth factors (GFs), which are bioactive biomolecules secreted by cells and can stimulate cell growth and differentiation, are commonly used. 3D printing of scaffolds containing a GF or GFs can be an effective strategy for successful tissue regeneration [13]. Transform growth factor β-1 in 3D printed structures was shown to accelerate cartilage

regeneration [14]. Vascular endothelial growth factors (VEGF) has been used in the regeneration of gastrointestinal tract [15] and vasculature [16]. In tissue engineering, it is highly important to control the release of GF from scaffolds in order to best promote tissue generation. Currently, there are mainly two approaches to incorporate growth factors into 3D printed scaffolds. One approach is to directly include growth factors in materials for 3D printing, and the other is to incorporate growth factors into delivery vehicles such as microspheres and nanofibers which are then included in materials for 3D printing. Either approach can be used, depending on the 3D printing technique, targeted tissue engineering application, and also other factors. Therefore, it is of great importance to develop a novel strategy to fabricate porous scaffolds with self-folding ability and controlled release of GF, which will overcome aforementioned difficulties to fabricate tubular porous structure and also produce scaffolds with desired shape morphing ability and GF delivery capability, as well as facilitating the formation of a layer of cells homogenously distributed on printed tubular scaffolds.

Poly(D,L-lactide-co-trimethylene carbonate) (PDLLA-*co*-TMC) is a temperature responsive polymer with a glass transition temperature close to 37 °C [17]. However, PDLLA-*co*-TMC is a synthetic polymer with which it is difficult to achieve direct cell attachment. GelMA is a natural hydrogel obtained by modifying gelatin with the methacryloyl group, and it keeps arginine-glycine-aspartic acid (RGD) peptide which facilitates cell attachment and promotes proliferation [18]. PDLLA-*co*-TMC and GelMA may be used together in 4D printing to form shape morphing scaffolds with desired shape morphing ability and good biological properties. Bilayer structures composed of a shape memory layer and a functional layer have been shown effective in both changing shapes and providing functions [19, 20]. In this work, a new strategy was developed to fabricate porous bilayer shape morphing scaffolds which could automatically change from the planar shape to tubular shape upon heating to the human body

temperature and provide controlled release of VEGF from the scaffolds. The term "porous" refers to the "macropores" in printed structures as in this study, both the PDLLA-*co*-TMC layer and GelMA layer are intended to have this type of pores, like in porous scaffolds produced by conventional technologies. The bilayer scaffolds were designed and fabricated by combining a shape morphing porous scaffold layer, which would be made by PDLLA-*co*-TMC to provide the whole bilayer scaffold with the shape change ability, and a functional porous scaffold layer, which would be made by GelMA hydrogel to carry VEGF for its controlled release in applications. The morphological properties and shape morphing behavior of both single-layer PDLLA-*co*-TMC scaffolds and bilayer PDLLA-*co*-TMC/GelMA scaffolds were investigated. The *in vitro* release behavior of VEGF from bilayer PDLLA-*co*-TMC/GelMA scaffolds crosslinked by an Ultraviolet (UV) light was also assessed. The effect of VEGF release on cells were studied using rat mesenchymal stem cells (rMSCs) that were seeded on bilayer scaffolds.

2. Materials and Methods

2.1. Materials

PDLLA-*co*-TMC with a DLLA:TMC molar ratio of 90:10 (inherent viscosity: 0.8 dL/g) was purchased from Daigang Biomaterials, Jinan, China. GelMA was synthesized using Van Den Bulcke *et al.*'s method [21]. Briefly, gelatin (type A from porcine skin, by Sigma-Aldrich) (10 g) was firstly dissolved in phosphate-buffered saline (PBS) (100 ml) at 50 °C. 0.8 ml methacrylic anhydride (MA) (a Sigma-Aldrich product) was then added into the gelatin solution under magnetic stirring and the reaction was continued for 3 to 4 hours. After completion of the reaction, the mixture was dialyzed against deionized water using a dialysis tubing for a week at 40 °C. Finally, the mixture was put in 50 ml tubes and freeze-dried for 5 days and was stored at -20 °C for future use. The synthesized GelMA was analysed by using

a Fourier transform infrared (FTIR) spectrometer (Bruker Tensor 27, USA). VEGF (recombinant human VEGF165, $\overline{Mw}$ = 38.2 kDa) and corresponding enzyme-linked immunosorbent assay (ELISA) kit (Human VEGF165 Standard ABTS ELISA Development Kit) were purchased from Peprotech, NJ, USA. All other chemicals were products of Sigma-Aldrich, USA, and used without further purification.

2.2. 3D printing of porous scaffolds

The fabrication of porous scaffolds, as illustrated in Fig. 1, was performed using a 3D bioprinter (3D Discovery™ Evolution, regenHU Ltd, Switzerland). The first step was to construct single-layer PDLLA-*co*-TMC shape morphing scaffolds via 3D printing (Fig.1a). Briefly, a certain amount of PDLLA-*co*-TMC was fully dissolved in dichloromethane (DCM, Applied Biosystems, Ireland) to obtain a 25% (w/v) PDLLA-*co*-TMC solution. The PDLLA-*co*-TMC solution was extruded onto a glass plate through 3D printing to form porous planar structures. The extrusion rate was controlled by changing the air pressure (0.5~0.8 bar), the layer thickness was set as 0.1 mm, the printing speed was 10 mm/s and the inner diameter of the nozzle of the printing head was 0.21 mm (27 G). After printing, the porous planar structures were dried at 25 ºC for 24 h to completely remove the organic solvent DCM. Afterwards, the planar structures were shaped into porous tubular structures by using a glass rod as a template in an oven (80 °C) for 90 mins. As such, the permanent shape of the PDLLA-*co*-TMC porous structures was defined. Glass rods of different diameters could be used as the template and hence the diameter of the formed tubular porous structures could be changed. Because PDLLA-*co*-TMC is naturally amorphous, the shaping process in the 80°C oven would cause a temperature gradient increasing from the surface to the interior of tubular scaffolds, which influences the degree of molecular orientation, leading to anisotropic birefringence and inhomogeneous transparency, which would result in the self-folding ability

of PDLLA-*co*-TMC structures [22]. The second step was to construct bilayer shape morphing scaffolds as shown in Fig.1b. The porous tubular PDLLA-*co*-TMC structure was flattened at 25°C and coated with a layer of alginate which would serve as a natural glue to bind the PDLLA-*co*-TMC layer and the subsequent GelMA hydrogel layer. 10% w/v GelMA hydrogel loaded with VEGF (2 μg/ml) was then printed onto the PDLLA-*co*-TMC porous scaffold layer, followed by crosslinking of GelMA via exposure to a UV light at the wavelength of 365 mm for 90s or 180s from a UV irradiation system (UVP 3UVTM Lamp, Analytic Jena, USA), thereby forming planar bilayer PDLLA-*co*-TMC/GelMA-VEGF scaffolds.

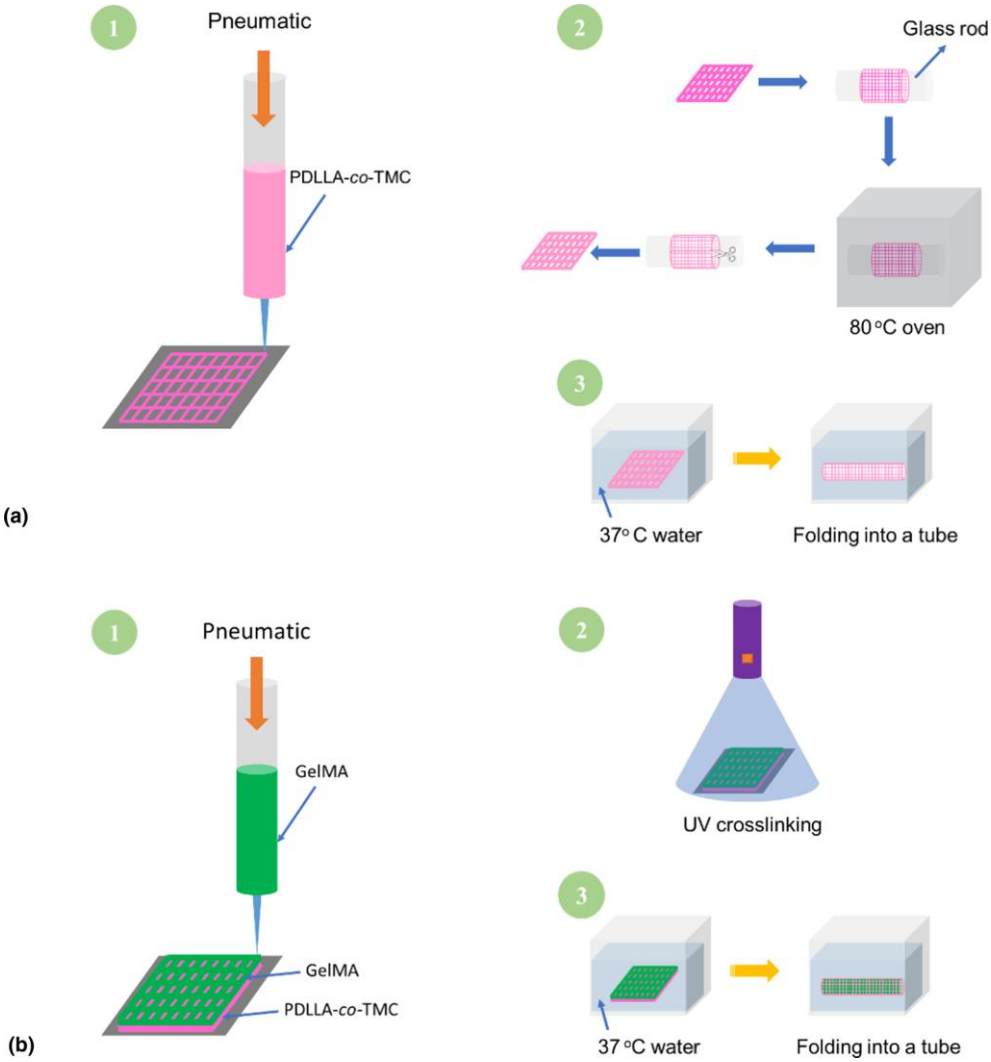

Figure 1. Schematic illustrations of 3D printing for the fabrication of porous shape morphing scaffolds and their self-folding upon heating: (a) fabrication of single-layer PDLLA-*co*-TMC self-folding scaffolds; (b) fabrication of bilayer PDLLA-*co*-TMC/GelMA self-folding scaffolds by printing a GelMA scaffold onto flattened PDLLA-*co*-TMC scaffold.

2.3. Morphological and structural characterization

The morphology and structure of both single-layer PDLLA-*co*-TMC scaffolds and bilayer PDLLA-*co*-TMC/GelMA scaffolds at their permanent tubular shapes were studied using a field emission scanning electron microscope (Hitachi S3400N VP SEM, Japan). The 3D printed scaffold specimens for SEM observations were freeze-dried and then sputter-coated with a thin layer of gold. SEM images of the surface and cross-sections of both types of scaffolds were recorded, showing the surface morphology and cross-section views of single-layer or bilayer scaffolds.

2.4. Shape morphing behaviour of 3D printed porous scaffolds

The shape morphing behaviour of single-layer PDLLA-*co*-TMC scaffolds and bilayer PDLLA-*co*-TMC/GelMA scaffolds was investigated by placing them in their temporary 2D planar shape in a still water tank at 37 ºC. Their shape evolution processes were recorded using a digital camera.

2.5. *In vitro* growth factor release

The *in vitro* release behaviour of VEGF loaded in bilayer PDLLA-*co*-TMC/GelMA scaffolds with different UV crosslinking times (90s or 180s) was studied through *in vitro* release tests using the VEGF ELISA kit. In a typical *in vitro* release test, scaffold samples were put into individual plastic tubes filled with an immersion liquid that was prepared from PBS (pH 7.4)

supplemented by 0.02% w/v sodium azide, 0.05% v/v Tween-20 and 0.5% w/v bovine serum albumin. The plastic tubes were then put in a shaking water bath at 37 ºC for up to 21 days for VEGF release. At each pre-determined time point, the immersion liquid was collected for analysis and replaced with freshly prepared immersion liquid. The VEGF concentration in the collected liquids was measured in a 96-well plate using the VEGF ELISA kit according to the manufacturer's protocol, while solutions of different VEGF concentrations were prepared and their concentrations were measured for establishing the standard curve. Each well was incubated at 25 ºC for colour development, which was then analyzed using an ELISA plate reader (UVM 340, Asys HiTech GmbH) at a measuring wavelength of 405 nm and a reference wavelength of 650 nm. The VEGF concentration measurements were made in triplicate. The VEGF concentration in each collected immersion liquid was calculated according to the standard curve and then used to establish cumulative release profiles of VEGF for the different bilayer scaffolds.

2.6. *In vitro* biological study

To investigate the influence of VEGF release on cell behaviour, rMSCs were cultured with bilayer shape morphing scaffolds with or without VEGF incorporation. Before cell seeding on scaffolds, rMSCs were cultured in the cell culture medium under 5% CO_2 at 37 ºC. After several days of culture, the cells were detached and counted, followed by seeding the cells at a cell density of 1.5×10^5 cells/cm^2 on the GelMA side of sterilized bilayer scaffolds with or without VEGF incorporation in a 24-well-plate. After 3-day culture, the cell viability was examined using LIVE/DEAD assay. Cell-scaffold samples were washed three times using sterilized PBS and then stained with ethidium homodimer EthD-1 for dead cells, which would show red fluorescence, and with calcein AM for living cells, which would show green fluorescence. Fluorescence images of the cell-scaffold structures were obtained using a

fluorescence microscope (Nikon Eclipse TE2000-U inverted microscope, Japan). Cell proliferation was qualitatively assessed through the fluorescence images.

3. Results and Discussion

3.1. 3D printing, morphology and structure of porous shape morphing scaffolds

The porous shape morphing scaffolds were designed as a bilayer structure where PDLLA-*co*-TMC with shape memory property was to be printed as the outer scaffold layer to provide the shape morphing ability upon heating while GelMA hydrogel was to be printed as the inner scaffold layer to provide the GF-delivery function for the scaffolds. The first step in production was to fabricate single-layer of PDLLA-*co*-TMC scaffolds by directly extruding the PDLLA-*co*-TMC solution onto the build platform which was coatied with a thin layer of Vaseline for easily detachment of the printed structures (Fig.1a). The 3D printed planar PDLLA-*co*-TMC scaffolds were then shaped into tubular scaffolds on a glass rod at 80 ºC. Glass rods of different diameters could be used, depending on the diameter of the tubular scaffolds that were aimed to produce. In the current investigation, a glass rod with a diameter of 7.5 mm was used. After shaping, the tubular scaffolds were cut from the glass rod, flatten, and remained in the temporary planar shape at 25 ºC (Figs.2a and 2b). The planar PDLLA-*co*-TMC porous scaffolds were put in a water tank at 37 ºC and could self-fold into the permanent tubular shape with a diameter of about 7.5 mm (Figs.2e and 2f). To examine the morphology and structure of scaffolds, single-layer PDLLA-*co*-TMC scaffolds in the permanent tubular shape were imaged under SEM. As could be seen, there were macropores regularly appearing on the surface of PDLLA-*co*-TMC scaffolds (Fig.2i, the top view of a scaffold) and a circle structure of scaffolds was revealed from the side view(Fig.2j), demonstrating good structural features of 3D printed single-layer PDLLA-*co*-TMC scaffolds.

To obtain the final bilayer shape morphing scaffolds, GelMA was subsequently printed on planar PDLLA-*co*-TMC scaffolds (Fig.1b). The 3D printed porous GelMA scaffold adhered tightly to the 3D printed porous PDLLA-*co*-TMC scaffold via a high-viscosity alginate glue. This was because anionic alginate and cationic GelMA could form strong interface adhesion through the ionic interaction between two oppositely charged hydrogels [23]. After 3D printing, the bilayer PDLLA-*co*-TMC/GelMA scaffolds thus formed were immersed in a $CaCl_2$ solution (5% w/v) for a short time (about 10 s) for alginate crosslinking. Alginate is a polysaccharide which has good biocompatibility and undergoes rapid gelation in the presence of divalent cations such as Ca^{2+} and hence is suitable for tissue engineering applications [24]. The resultant bilayer PDLLA-*co*-TMC/GelMA scaffolds, as shown in Figs.2c and 2d, could maintain the temporary planar shape at 25 ºC. After heating to 37 ºC, the bilayer scaffolds could also automatically fold into a tubular shape (Figs.2g and 2h). The structure and morphology of bilayer scaffolds in the permanent tubular shape was also observed using SEM. The GelMA scaffold layer (having a thickness of about 30 μm) within bilayer scaffolds was visualized through the macropores from the top view of scaffolds (Fig.2k) and was shown to stably bond to the outer scaffold layer of PDLLA-*co*-TMC (having a thickness of about 90 μm) from the side view of scaffolds (Fig.2l), suggesting the successful fabrication of porous bilayer shape morphing scaffolds.

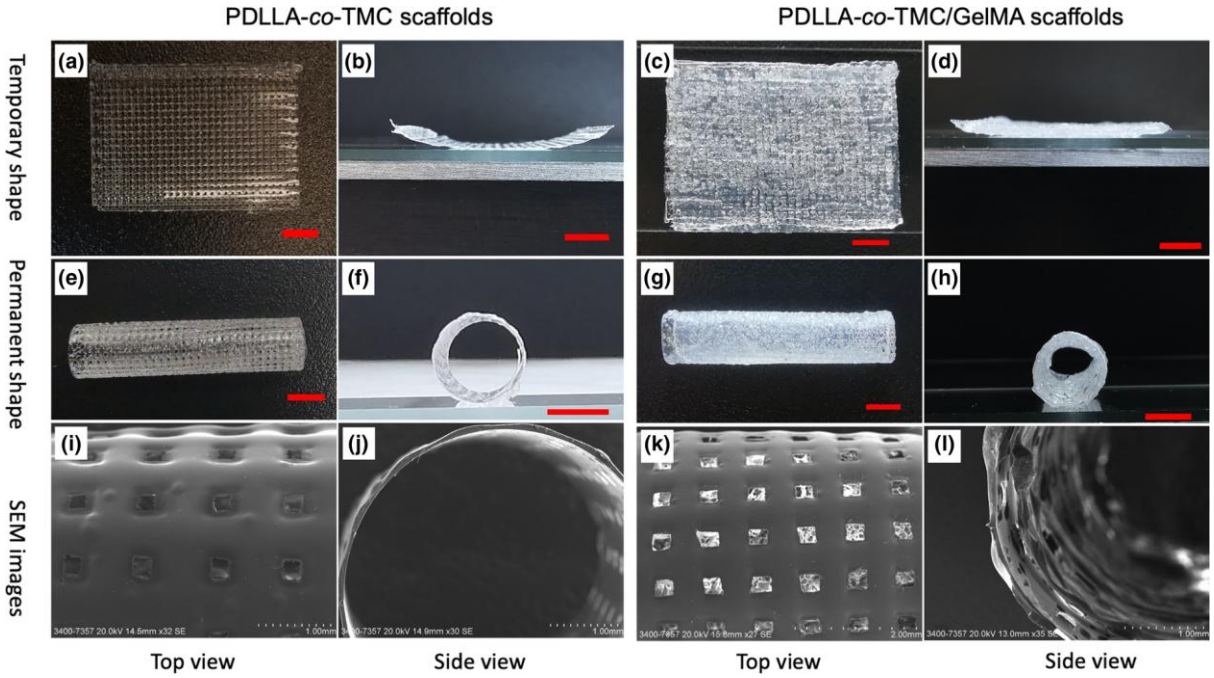

Figure 2. Morphology and structure of 3D printed porous shape morphing scaffolds: (a, b, e, f) photographs of single-layer PDLLA-*co*-TMC scaffolds showing the temporary shape at 25 ºC and permanent shape at 37 ºC with both top view and side view, and (i, j) SEM images of single-layer PDLLA-*co*-TMC scaffolds in the permanent tubular shape with both top view and side view; (c, d, g, h) photographs of bilayer PDLLA-*co*-TMC/GelMA scaffolds showing the temporary shape at 25 ºC and permanent shape at 37 ºC with both top view and side view, and (k, l) SEM images of bilayer PDLLA-*co*-TMC/GelMA scaffolds in the permanent tubular shape with both top view and side view. (Scale bar: 5 mm.)

3.2. Shape morphing behavior of 3D printed porous scaffolds

Excellent shape morphing ability of 3D printed scaffolds is important for their clinical applications where a shape memory scaffold should keep its temporary shape stably at room temperature while according to the programmed design, it should undergo shape change automatically at the body temperature after its implantation so as to match the tissue defect shape and size. It has been found that PDLLA-*co*-TMC with a PDLLA:TMC ratio of 9:1 has

a glass transition temperature T_g that is slightly higher than the body temperature of 37 ºC, which enables on-demand control over its shape recovery by applying direct heating or external thermal stimuli [17].

The shape morphing behavior of both single-layer PDLLA-*co*-TMC scaffolds and bilayer PDLLA-*co*-TMC/GelMA scaffolds were studied and compared. The scaffolds in the temporary planar shape were put into a 37 ºC water tank and could recover to their permanent tubular shapes automatically and quickly. As shown in Fig.3, when heated to 37 ºC by water, single-layer PDLLA-*co*-TMC scaffolds completed their shape memory circle within 37 s, while bilayer PDLLA-*co*-TMC/GelMA scaffolds could also evolve from their planar shape into tubular structures within 38 s, demonstrating the desired shape morphing ability. It appeared that adhering one layer of porous GelMA scaffold onto a porous PDLLA-*co*-TMC scaffold via alginate glue had little effect on the shape memory property of 3D printed PDLLA-*co*-TMC scaffold, indicating the success of our 3D printing strategy for forming bilayer porous shape morphing scaffolds for tissue engineering applications.

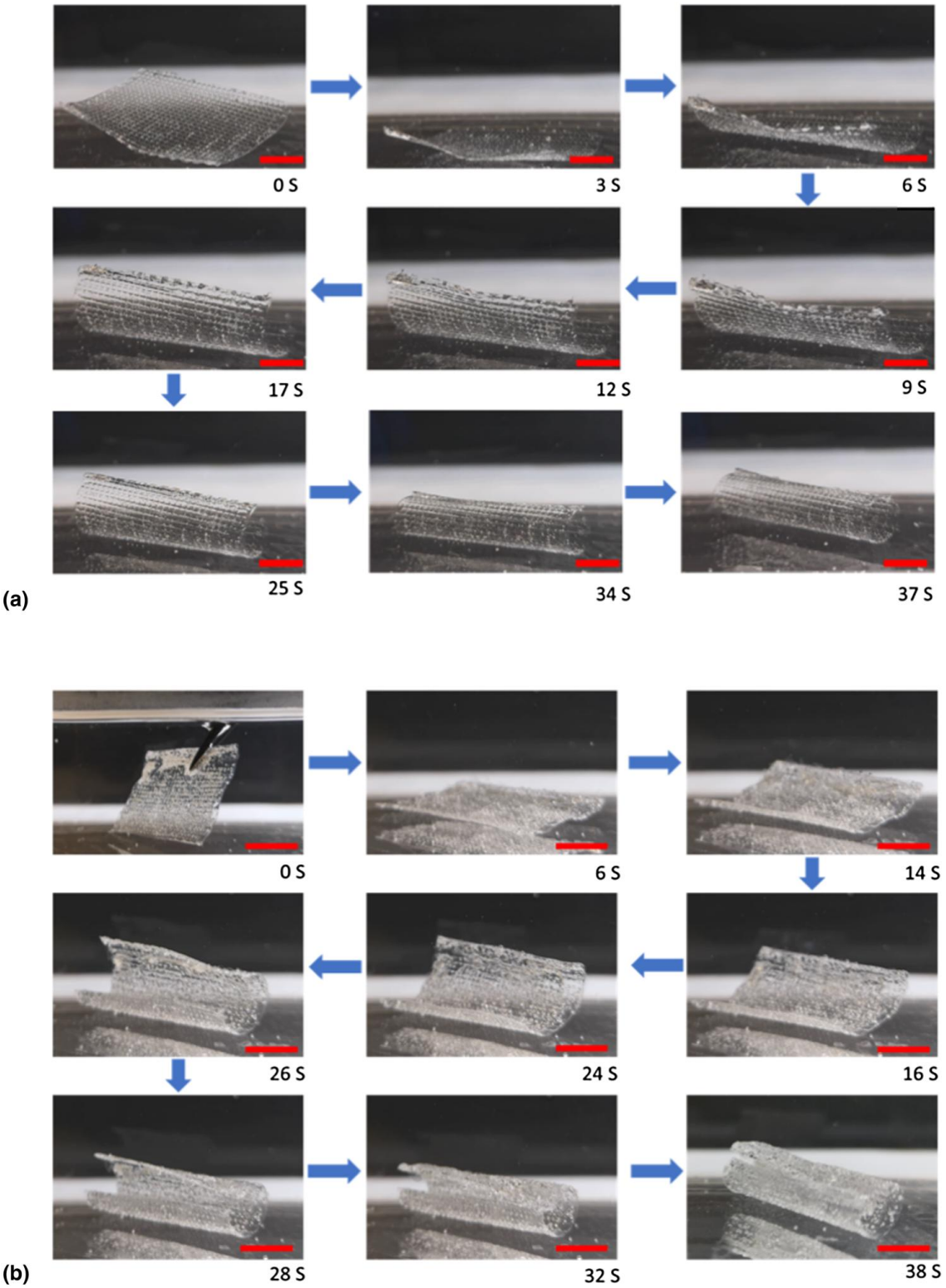

Figure 3. Shape morphing process of (a) single-layer PDLLA-*co*-TMC scaffolds, and (b) bilayer PDLLA-*co*-TMC/GelMA scaffolds. (Scale bar: 10 mm.)

3.3 Release of VEGF and its effect on cell behaviour

The release behaviour of VEGF from 3D printed porous shape morphing scaffolds with different photocrosslinking times (90 s or 180 s) was studied through *in vitro* release tests and it was observed that the scaffolds exhibited distinct release characteristics. As shown in Fig.4a, the overall release profiles of both shape morphing scaffolds displayed a two-stage release behaviour. In the first stage (for the initial three days), a quick release occurred, during which up to 30 to 50% of total amounts of encapsulated VEGF was released. The initial quick release of growth factors from 3D printed scaffolds is commonly observed for scaffolds encapsulated with different types of GFs [9, 25, 26], revealing a typical diffusion-controlled release behaviour. The quick release of VEGF could be attributed to the disassociation of VEGF molecules located on the surface of 3D printed shape morphing scaffolds into the immersion liquid. It should be noted that the initial release rate of bilayer shape morphing scaffolds with the 90 s crosslinking time was higher than that with the 180 s crosslinking time, which was mainly due to the lower structural integrity of GelMA crosslinked for 90 s and hence its faster degradation kinetics. In the second stage (after the initial three days), both shape morphing scaffolds exhibited a slower but steady release of VEGF until the end of *in vitro* release tests. The sustained release behaviour in this stage could be attributed mainly to the slow diffusion of VEGF molecules from the interior of GelMA matrix to the immersion liquid as well as the biodegradation of the GelMA functional scaffold layer. It was observed that after 21 days of *in vitro* release tests, shape morphing scaffolds with the 90 s crosslinking time had released about 60% of total VEGF loading while those with the 180 s crosslinking time had released significantly less VEGF (about 50% of total VEGF loading). With a shorter crosslinking time, the crosslinking degree of GelMA was lower and hence bilayer shape morphing scaffolds had a less stable structure in the simulated body environment, which led to faster degradation kinetics, and thus faster release of encapsulated VEGF. Therefore, as demonstrated, the release behaviour of VEGF from

porous bilayer shape morphing scaffolds could be manipulated by varying the crosslinking degree of GelMA which would be controlled by adjusting the crosslinking time.

To investigate the biocompatibility of 3D printed scaffolds and also the influence of VEGF release on cells, rMSCs were cultured on bilayer scaffolds with or without VEGF encapsulation. The viability of rMSCs on scaffolds was studied using LIVE/DEAD assay after 3-day culture with live cells stained green and dead cells stained red. As shown by fluorescence images (Fig.4b), rMSCs uniformly attached to both scaffolds and nearly all stained rMSCs on the scaffolds were live cells, indicating good biocompatibility of 3D printed PDLLA-*co*-TMC/GelMA scaffolds. Nearly all cells adhered to the GelMA layer of both scaffolds. This is because RGD peptide of GelMA had contributed to the cell attachment and proliferation. Also, it could be observed that PDLLA-*co*-TMC/GelMA scaffolds loaded with VEGF exhibited a much higher cell density than scaffolds without VEGF encapsulation (Fig.4b, top row), indicating that released VEGF from scaffolds had promoted the attachment and proliferation of rMSCs on the porous shape morphing scaffolds. VEGF is a growth factor and appears as homodimeric and heterodimeric polypeptides, which had further improved cell attachment and proliferation on the GelMA layer of bilayer scaffolds. At a higher magnification (10X, bottom row in Fig.4b), it was apparent that cells grown on PDLLA-*co*-TMC/GelMA-VEGF scaffolds became elongated and highly spreading whereas the cells grown on PDLLA-*co*-TMC/GelMA scaffolds were still rounded. These observations suggest that PDLLA-*co*-TMC/GelMA-VEGF scaffolds could effectively release encapsulated VEGF and that released VEGF could significantly promote cell growth. The results obtained in this study suggest that the porous shape morphing PDLLA-*co*-TMC/GelMA-VEGF scaffolds with control release of VEGF have great potential for the regeneration of tubular tissues such as vasculature and gastrointestinal tract.

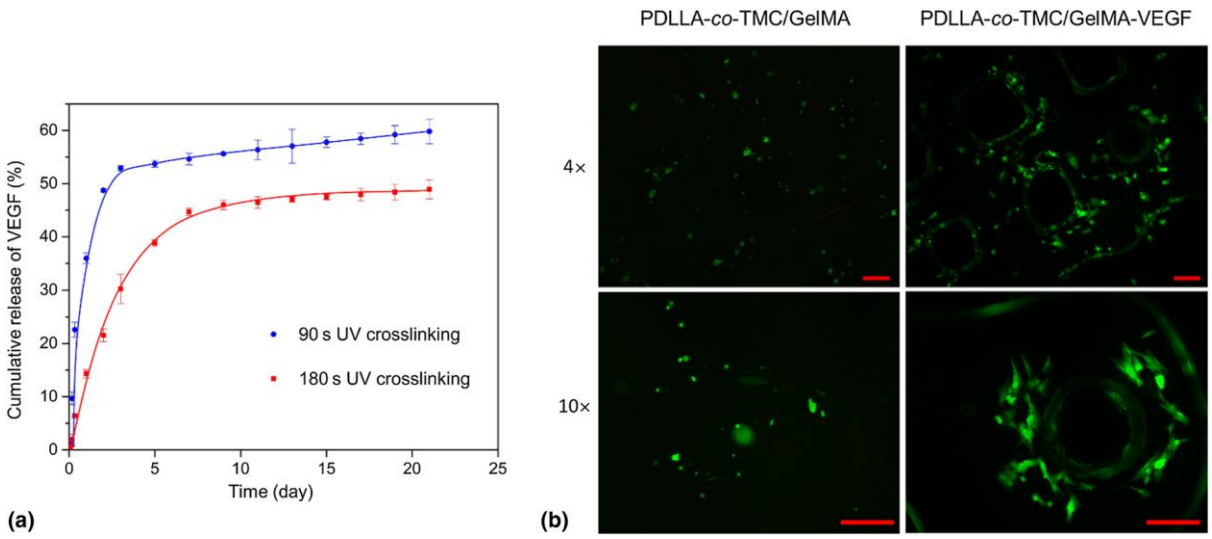

Figure 4. (a) *In vitro* release profiles of VEGF from shape morphing PDLLA-*co*-TMC/GelMA-VEGF bilayer scaffolds with different UV crosslinking times. (b) Fluorescence images (at 4X and 10X magnifications) of rMSCs seeded on shape morphing PDLLA-*co*-TMC/GelMA bilayer scaffolds with or without VEGF after 3-day culture. (Scale bar: 250 μm.)

The current study is basically a 4D printing investigation in tissue engineering. Furthermore, it is actually a half-a-step advance from 4D printing, i.e., 4.5D printing in tissue engineering, with the additional controlled GF release from 4D printed structures for tissue regeneration. With the encapsulation of VEGF, PDLLA-*co*-TMC/GelMA-VEGF scaffolds were made via 4.5D printing, endowing the PDLLA-*co*-TMC/GelMA scaffolds with an additional function of controlled GF delivery. The full 5D printing is developed from 4.5D printing and has been under investigation in our group. This work, together with the research conducted by others, contributes to the developments of printing technologies and strategies in the field.

4. Conclusions

This study developed a new strategy for fabricating porous bilayer scaffolds with self-folding ability and controlled release of growth factors via 3D printing. The bilayer scaffolds could

maintain the temporary planar shape at 25 ºC and upon heating to 37 ºC, automatically change to the permanent tubular shape very quickly owing to the shape memory property of the PDLLA-*co*-TMC scaffold layer. The 3D printed scaffolds had regular, designed pores and the two scaffold layers in bilayer scaffolds were tightly bonded. VEGF loaded in the shape morphing scaffolds showed a quick release in the initial 3 days, followed by a steady and sustained release within the test period of 21 days. The overall release profile of VEGF could be controlled by adjusting the photocrosslinking time of the GelMA scaffold layer that contained VEGF. PDLLA-*co*-TMC/GelMA bilayer scaffolds loaded with VEGF were biocompatible and conducive to cell attachment and proliferation. This work paves the way for further development of 4D printing in tissue engineering.

Acknowledgements

J. Lai and J. Li thank The University of Hong Kong (HKU) for awarding them with research scholarships at HKU. This work was financially supported by Hong Kong Research Grants Council (RGC) through a GRF research grant (17201017) and by HKU through a Seed Fund for Basic Research grant. Assistance provided by members in M. Wang's group and by technical staff in HKU's Department of Mechanical Engineering, Faculty of Dentistry and Electron Microscopy Unit is acknowledged.

Supplementary Material Available: FTIR spectrum of synthesized GelMA.

References

1. C. Wang, Q. Zhao, and M. Wang: Cryogenic 3D printing for producing hierarchical porous and rhBMP-2-loaded Ca-P/PLLA nanocomposite scaffolds for bone tissue engineering. *Biofabrication*. **9**, 025031 (2017).
2. B. Duan and M. Wang: Selective laser sintering and its biomedical applications, in *Laser Technology in Biomimetics*. 83 (2013).
3. C.W. Hull: Apparatus for production of three-dimensional objects by stereolithography. US Patents, 45,753,301 (1986).
4. S.C. Ligon, R. Liska, J. Stampfl, M. Gurr, and R. Mulhaupt: Polymers for 3D Printing and Customized Additive Manufacturing, *Chem. Rev.* 10212 (2017).
5. C.K. Chua and W.Y. Yeong: Bioprinting: principles and applications. *World Scientific Publishing Co Inc.* **1**, (2014)
6. V.M. Sean, and A. Anthony: 3D bioprinting of tissues and organs. *Nat. Biotechnol*. **32**, 773 (2014).
7. S. Tibbits: The emergence of "4D printing". in *TED conference*. 2013.
8. Z. Wan, P. Zhang, Y. Liu, L. Lv, and Y. Zhou: Four-dimensional bioprinting: Current developments and applications in bone tissue engineering. *Acta Biomater*. (2019).
9. C. Wang, Y. Zhou, and M. Wang: In situ delivery of rhBMP-2 in surface porous shape memory scaffolds developed through cryogenic 3D plotting. *Mater. Lett*. **189**, 140 (2017).
10. S. Miao, W. Zhu, N.J. Castro, M. Nowicki, X. Zhou, H. Cui, J.P. Fisher, and L.G. Zhang: 4D printing smart biomedical scaffolds with novel soybean oil epoxidized acrylate. *Sci. Rep*. **6**, 27226 (2016).
11. M. Zarek, N. Mansour, S. Shapira, and D. Cohn: 4D Printing of Shape Memory-Based Personalized Endoluminal Medical Devices. *Macromol. Rapid Commun*. **38**, 1600628 (2017).
12. L. Zhang, Y. Xiang, H. Zhang, L. Cheng, X. Mao, N. An, L. Zhang, J. Zhou, L. Deng, and Y. Zhang: A Biomimetic 3D-Self-Forming Approach for Microvascular Scaffolds. *Adv. Sci*. 1903553 (2020).
13. G.L. Koons, and A.G. Mikos: Progress in three-dimensional printing with growth factors. *J. Controlled Release*. **295**, 50-59 (2019).
14. L.K. Narayanan, P. Huebner, M.B. Fisher, J.T. Spang, B. Starly, and R.A. Shirwaiker: 3D-bioprinting of polylactic acid (PLA) nanofiber–alginate hydrogel bioink containing human adipose-derived stem cells. *ACS Biomater. Sci. Eng.* **2**, 1732 (2016)
15. Y. Zhou, Q. Zhao, and M. Wang: Dual release of VEGF and PDGF from emulsion electrospun bilayer scaffolds consisting of orthogonally aligned nanofibers for gastrointestinal tract regeneration. *MRS Commun*. **9**, 1098 (2019).
16. M.T. Poldervaart, H. Gremmels, K. van Deventer, J.O. Fledderus, F.C. Öner, M.C. Verhaar, W.J. Dhert, and J. Alblas: Prolonged presence of VEGF promotes vascularization in 3D bioprinted scaffolds with defined architecture. *J. Control Release*. **184**, 58 (2014).
17. M. Bao, X. Lou, Q. Zhou, W. Dong, H. Yuan, and Y. Zhang: Electrospun biomimetic fibrous scaffold from shape memory polymer of PDLLA-co-TMC for bone tissue engineering. *ACS Appl. Mater. Inter*. **6**, 2611-2621 (2014).
18. K. Yue, G. Trujillo-de Santiago, M.M. Alvarez, A. Tamayol, N. Annabi, and A. Khademhosseini: Synthesis, properties, and biomedical applications of gelatin methacryloyl (GelMA) hydrogels. *Biomaterials*. **73**, 254-271 (2015).
19. X. Du, H. Cui, B. Sun, J. Wang, Q. Zhao, K. Xia, T. Wu, and M.S. Humayun: Photothermally Triggered Shape-Adaptable 3D Flexible Electronics. *Adv. Mater. Technol*. **2**, 1700120 (2017).
20. W. Wang, C. Li, M. Cho, and S. H. Ahn: Soft tendril-inspired grippers: shape morphing of programmable polymer–paper bilayer composites. *ACS Appl. Mater. Inter*. **10**, 10419-10427 (2018).
21. A.I. Van Den Bulcke, B. Bogdanov, N. De Rooze, E.H. Schacht, M. Cornelissen, and H. Berghmans: Structural and rheological properties of methacrylamide modified gelatin hydrogels. *Biomacromolecules*. **1**, 31 (2000).

22. L. Struik: Orientation effects and cooling stresses in amorphous polymers. *Polym. Eng. Sci.* **18**, 799-811 (1978).

23. H. Li, Y.J. Tan, S. Liu, and L. Li: Three-dimensional bioprinting of oppositely charged hydrogels with super strong interface bonding. *ACS Appl. Mater. Interfaces*. **10**, 11164 (2018).

24. K.Y. Lee and D.J. Mooney: Alginate: properties and biomedical applications. *Prog. Polym. Sci.* **37**, 106 (2012).

25. J.Y. Park, J.H. Shim, S.A. Choi, J. Jang, M. Kim, S.H. Lee, and D.W. Cho: 3D printing technology to control BMP-2 and VEGF delivery spatially and temporally to promote large-volume bone regeneration. *J. Mater. Chem. B*. **3**, 5415 (2015).

26. W. Zhu, H. Cui, B. Boualam, F. Masood, E. Flynn, R.D. Rao, Z.Y. Zhang, and L.G. Zhang: 3D bioprinting mesenchymal stem cell-laden construct with core–shell nanospheres for cartilage tissue engineering. *Nanotechnology*. **29**, 185101 (2018).